Int. J. Nano Dimens., 13 (1): 71-86, Winter 2022

ORIGINAL ARTICLE

Study of phosphorene nanoribbon for making nanotube selective gas sensor

*Hossein Bahmani Kazerooni, Rahim Ghayour *, Farshad Pesaran*

Department of Electrical Engineering, Shiraz Branch, Islamic Azad University, Shiraz, Iran

Received 03 July 2021; revised 04 August 2021; accepted 04 August 2021; available online 12 August 2021

Abstract

Phosphorene nanoribbon (PNR) is a two-dimensional crystalline substance possessing semiconductor property, which makes it a new promising gas sensor. The gas sensing performance significantly depends on the adsorption mechanism and the strength of bonding between gas molecules and phosphorene atoms. Adsorption of a gas molecule onto PNR can be investigated through different parameters, such as interatomic energy, distance between atoms, and changes in the band gap energy of PNR. In this research, first, the PNR relaxation is carried out for minimum energy of whole structure. Second, the folding and tubing of PNR are investigated for their stability and minimum energy specification. Next, we constructed a phosphorene nanotube (PNT) by connecting two folded PNR that we called it unconventional PNT (UPNT). We compared conventional cylindrical PNT (CPNT) with UPNT for their energies and electrical properties. In the final step, as gas nanosensor, the gas sensing behavior and specifications of CPNT and UPNT are investigated in the presence of several gases. Since a phosphorene nanotube generally has a stable structure, the presence of gas molecules causes deformation of crystalline of structure and change in its electronic properties. For evaluating the sensing properties of CPNT and UPNT, their I-V characteristics, density of states and energy band diagrams are calculated and compared in the absence and presence of gas molecules. The adsorption of CO, CO_2, NH_3, NH, and O_2 gas molecules onto UPNT and CPNT are done in detail. The results show that the sensitivity of UPNT gas sensor is higher than that of CPNT for detecting special gas molecules. We further investigated the amount of charge transfer utilizing the nonequilibrium Green's function (NEGF) formalism which is applied on crystallized atomic configuration.

Keywords: *Density Functional Theory (DFT); Gas Sensor; Nonequilibrium Green's Function (NEGF); Phosphorene Nanoribbon (PNR); Phosphorene Nanotube (PNT).*

How to cite this article

Bahmani Kazerooni H., Ghayour R., Pesaran F. Study of phosphorene nanoribbon for making nanotube selective gas sensor . Int. J. Nano Dimens., 2022; 13(1): 71-86.

INTRODUCTION

Two-dimensional (2D) crystalline nanosheets developed by a solitary or epitaxy of few nuclear layers, for example, graphene and metal di-chalcogenides (e.g. MoS_2), introduce an emerging class of materials in recent years. These sheets have gained interest in light of their unique structures related to expansive surface zones and many dynamic destinations [1-4]. The advantages of these materials, nonetheless, are restrained by some characteristic deficiencies like the absence of a band gap in graphene and moderately low flexibility in MoS_2 [5], which pushed research on 2D materials with properties that may prompt explicit improved execution [6-8].

Fig. 1 shows the atomic structure of black phosphorus (BP) [9-11]. The shape of the crystalline formation of black phosphorus shown in Fig.1 extracted through crystalline relaxation by utilizing density functional theory computations. The construction is layered and consists of sheets of the phosphorus atoms which are arranged in a lattice of puckered honeycomb shape. In analogy to the name of graphene, the monolayer or few-layer crystalline back phosphorous is named

* Corresponding Author Email: *rghayour@shirazu.ac.ir*

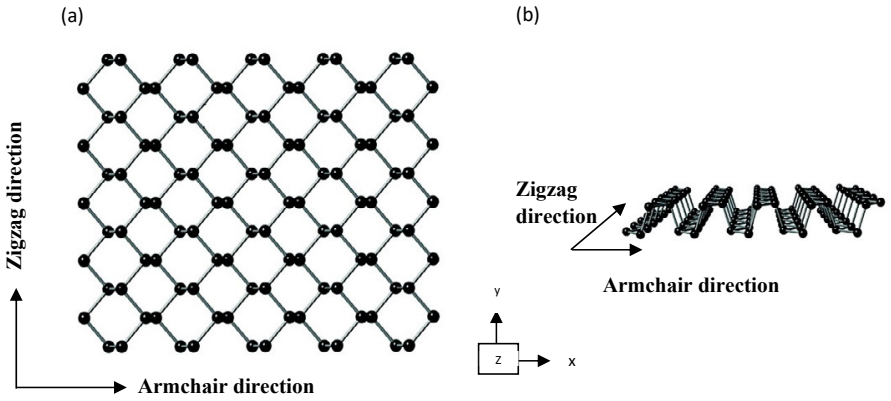

Fig. 1. Black phosphorus structure. (a) mono layer phosphorene nanoribbon from top view, (b) mono layer black phosphorus structure from side view [9].

phosphorene [9]. As depicted in Fig. 1(a), in monolayer phosphorene, each one atom bonds with three nearby phosphorus atoms and this honeycomb puckered network is shaped by sp^3 hybridization which is due to the phosphorus particles has three electrons in valance band[12]. The single layers of phosphorus atoms are tied together by van der Waals (vdW) forces which are weak and vdW interactions are dominant along the crystallographic y orientation [13]. The x and y directions in the BP structure are matched with the armchair and the zigzag directions, respectively, where the result of in-plane anisotropy is very unique within these two directions (Fig. 1(b)). In fact, some physical parameters, such as effective mass and group velocity strongly depend on the direction of atomic conFiguration of BP [14].

Phosphorene has a useful behavior similar to graphene such as limited and direct bandgap within the energy range required for electronic devices. Furthermore, phosphorene displays other valuable properties, optical counting applications and anisotropic electric conductance which differentiate it from other isotropic 2D materials like graphene [9, 10]. These properties are useful for realizing significant utilizations in the field-effect transistor (FET) [6] and slender film sun oriented cells [15].

Two-dimensional materials typically provide great possibility as gas sensors because of their great surface to volume proportion and their appropriate charge exchange between gas molecules and the substrates [16]. In phosphorene case, it is demonstrated that the gas molecule adsorption actuates the charge carrier which can be utilized to make more sensitive sensors. The sensor property depends on changes in the device resistivity due to presence and absence of gas atoms [16].

The particular electronic properties of phosphorene that is profoundly attractive are the influences of gas atom adsorption on the electrical behavior of phosphorene. Also, we need to evaluate unmistakable attributes of the impact of atoms or molecules on the carrier transport and electrical conduction. In the following sections, we introduce two phosphorene nanotube (PNT) structures and show their behaviors due to gas absorption. Using pseudo potential-density-functional-theory calculations, we show that folded structure alters the electronic band structure of phosphorene. We also demonstrate the ways to find the best atomic conFiguration (position of atoms) of PNTs to achieve a fully relaxed structure.

In the following, first, the electrical properties of conventional and folded zigzag PNRs are investigated. We propose a structure consists of connected two folded PNRs which makes an unconventional phosphorene nanotube (we called it UPNT). Then, comparisons of UPNT and a conventional PNT (CPNT) for their electrical properties and their gases adsorptions are done in detail. The sensitivities of gases sensors are performed by calculating I-V characteristics of each sensor in presence and absence of different gases.

Calculations are done utilizing a nonequilibrium Green's function (NEGF) formalism. The results show that the sensitivity and selectivity of the UPNT gas sensor in presence of special gas molecules are higher than those of CPNT cases.

Additionally we calculated the charge transfer relations using the NEGF formalism. However, in both CPNT and UPNT structures, the kind of gas molecules significantly changes the charge transfer along the sensor. Finally, it is to be noted that at all stages of this study; we focused on examining the process of changes in electrical properties of each structure due to gas adsorption.

MATERIALS AND METHODS

Based on density functional theory, the first-principle calculations are performed by utilizing the Plane-Wave Self-Consistent Field (PWSCF) program of the Quantum-ESPRESSO open source distribution [17]. The ultra-soft pseudo-potential [18] and general gradient approximation are applied to take the advantage of the Perdew-Becke-Ernzerhof (PBE) formula [19]. The procedure is followed for the exchange and correlation of energy functions until the total interatomic forces becomes less than 0.04eV/A^2 [20, 21].

The total energy transfer between a gas molecule and the graphene nanoribbon is determined as the adsorption energy and signified by E_{Total}. A negative value of E_{Total} comprises a stable adsorption and it should be noted that a larger negative value (i.e. greater absolute value) of E_{Total} results in a more stable bonding formation [21].

Van der Waals (vdW) interactions or interlayer interactions in 2D materials, has affluent effects on the physical properties of layered materials [13]. Due to the crystalline structure of black phosphorus, the vdW modification proposed by Grimme (DFT-D2) is incorporated in the computations [22, 23]. Bilayer phosphorene is modeled by utilizing slabs, which are splitted by a vacuum layer with an approximate thickness of 35A° [24]. For electronic computations, in order to obtain more accurate electron-phonon interaction matrices, Brillouin zone integrations [25] are accomplished with (1, 1, 12) grid mesh in the wave vector k space using the Monkhorst-Pack K-point technique [26]. By taking advantage of the linear response theory, the Fourier interpolated through the full Brillouin zone and dynamical matrices are calculated for special K-points in the 2D irreducible Brillouin zone [27, 28]. Electronic transport properties and I-V relations are obtained by NEGF procedures inside the Keldysh formalism which is done in the TRANSIESTA package [29, 30]. The current of electrons through the Phosphorene nanoribbon (PNR) between the contacts is determined using the Landauer-Buttiker formula as [31]:

$$I\left(V_b\right) = G_0 \int_{\mu_L}^{\mu_R} T\left(E, V_b\right) dE \quad (1)$$

where G_0 is the conductance quantum and $T(E,V_b)$ is the transmission eigenvalues of the channels at the energy E under a bias potential of V_b. The hydrogenated phosphorene nanosheet molecular device is developed using a 1 × 1 × 4 supercell, which displays a 2D clasping structure. The phosphorene nanoribbon as a conductive device comprises of three sections, namely scattering region, right electrode, and left electrode known as contacts. Just to better understand the subject, Fig. 2 is presented symbolically. Supposing to decrease the impact of dangling bonds on the edges of the phosphorene nanosheet, they are hydrogenated as shown in Fig. 3. In Fig. 2 the scattering region of the phosphorene nanostructure comprises of 48 phosphorus atoms. The left and right electrodes contain 16 phosphorus atoms each. The length of the phosphorene scattering region is 11.6 Å and the length of each left and right electrode is 3.97 Å.

The calculated current is recorded regarding

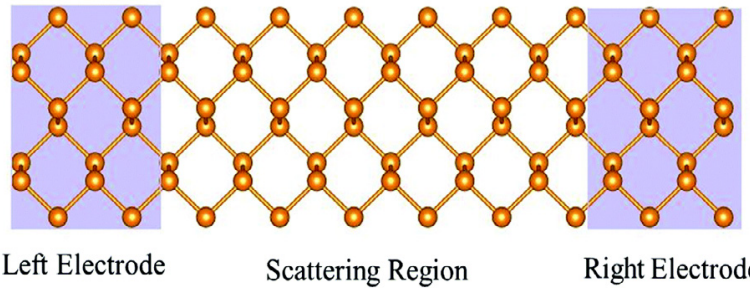

Fig. 2. Scattering region, left and right electrodes (contacts) of phosphorene nanoribbon, a set-up for I-V measurement.

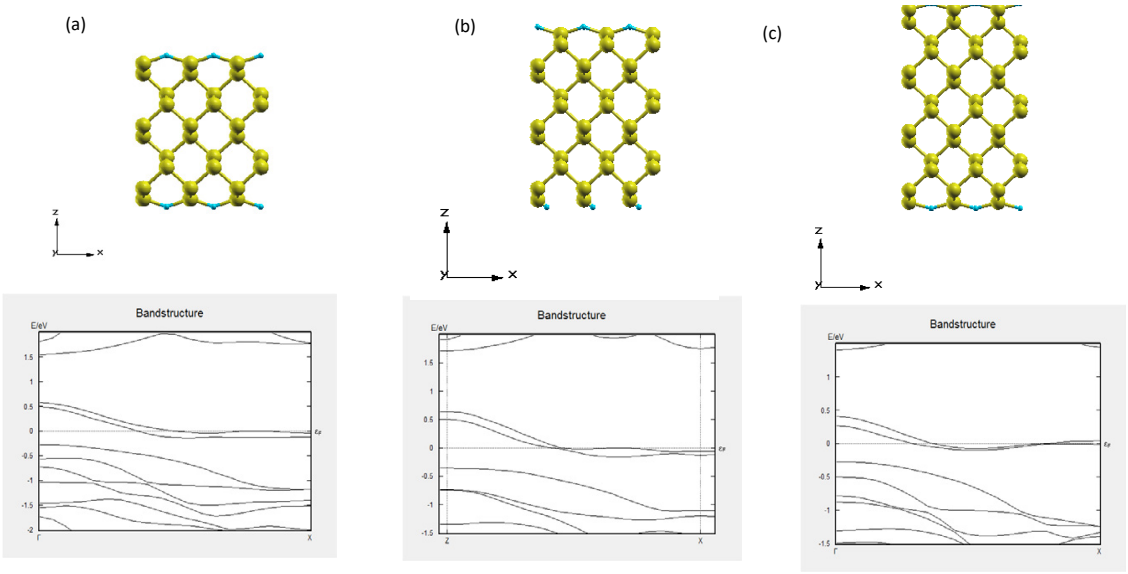

Fig. 3. Comparison of atomic structures and energy diagrams of zigzag phosphorene nanoribbons by changing the number of atoms across the nanoribbon width. Green and blue circles denote phosphorous and Hydrogen atoms, respectively. a) PNR with 3p–1 phosphorous atoms in the width: b) PNR with 3p phosphorous atoms in the width c) PNR with 3p+1 phosphorous atoms in the width (with the same p value).

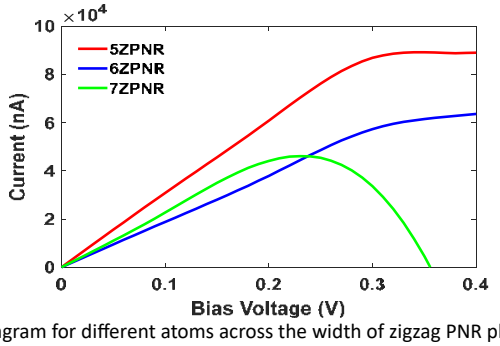

Fig. 4. Current-Voltage diagram for different atoms across the width of zigzag PNR phosphorene nanoribbons.

applied of bias voltage V, where the potential difference of $-\frac{V}{2}$ and $+\frac{V}{2}$ are kept across the left and right electrodes and the phosphorene molecular system as shown in Fig2.

RESULTS AND DISCUSSIONS

In this section, we first examine the atomic structures of zigzag phosphorene nanoribbons for the number of 3p-1, 3p, 3p+1 (for p=2) atoms across the width by applying relaxation process. Supposing to neutralize the boundary (edges) reactions on the device attitude, the phosphorous atoms located at the margins of nanoribbon are replaced by hydrogen atoms.

Pristine PNR versus folded PNR

Figs. 3(a, b, c) shows the PNR with 5, 6, 7 phosphorous atoms in width, respectively. We found that by increasing the number of atoms across the width of the nanoribbons, the amount of energy gap is reduced. Moreover, by changing the number of atoms in the width of PNR, the Fermi energy level (E_f), the energy level of the highest occupied molecular orbitals (EHOMO), the energy level of the lowest unoccupied molecular orbitals (ELUMO), the energy gap and thus the I-V characteristic change accordingly. To investigate I-V characteristics, we utilize a two-probe system where semi-infinite left and right electrode regions are intimately connected to the central scattering region as shown in Fig. 2. The relaxed structures are used in the electronic calculations at different bias voltages from 0V to 0.4V by 0.1 intervals. In Fig. 4, we have presented the I-V curves for different number of atoms across the width of zigzag PNR. Comparison of all the results are illustrated in Figs.

Table1. Comparison of energy properties of PNR and PNT with various atomic structure.

	Zigzag PNR with 5 (3p-1) atoms in width	Zigzag PNR with 6 (3p) atoms in width	Zigzag PNR with 7 (3p+1) atoms in width	Folded PNR with 20 atoms in width	Folded PNR with 28 atoms in width	Folded PNR with 20 atoms in width and 8.44A space between two arms	Folded PNR with 20 atoms in width and 5.83A space between two arms
Ef (eV)	-4.33	-4.31	-4.26	-3.87	-5.20	-3.87	-4.26
Eg (eV)	0.19	0.14	0.11	0	0	0	0
Ehomo (eV)	-4.68	-4.59	-4.53	-3.82	-5.15	-3.82	-4.26
Elumo (eV)	-4.49	-4.45	-4.35	-5.40	-6.73	-5.40	-4.42

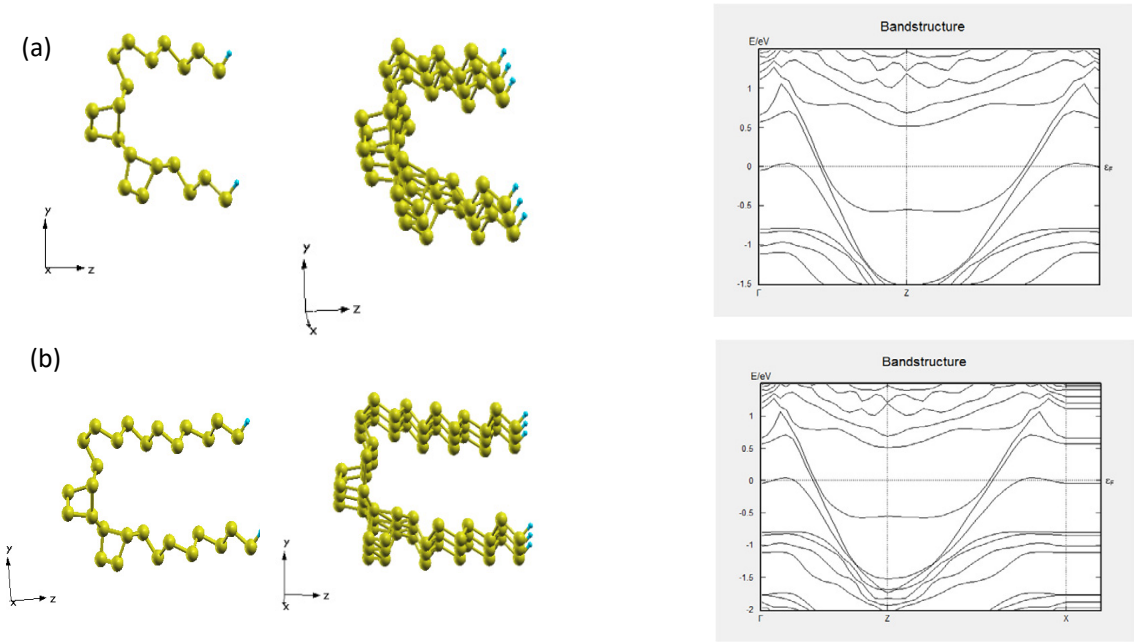

Fig. 5. Hydrogenated folded phosphorene nanoribbon with :
a) 20 phosphorous atoms: Ef=-3.87 eV EHOMO=-3.82 eV ELUMO=-5.40 eV , Eg=0eV
b) 28 phosphorous atoms: Ef=-5.20 eV EHomo=-5.15 eV ELumo=-6.73eV Eg=0eV.

3, 4 and summarized in Table 1.

We show that any change in the number of atoms in two arms of folded PNR modifies its atomic structure and the electronic specifications. Figs. 5(a, b) shows the simulation results of two stages with 20 and 28 atoms respectively. Another factor that changes the electronic and structural characteristics of the folded PNR is the change in the distance between two arms of the folded PNR. In Figs. 6(a, b) this problem is demonstrated for D= 8.44 Aº and D=5.83 Aº which the results are summarized in Table 1.

Pristine PNT

Now, by connecting two folded PNR to each other a proposed phosphorene nanotube known as unconventional PNT (UPNT) is obtained which shows in Figs. 7(a, b). It is interesting to compare it with a conventional PNT (CPNT) that is made by rolling a sheet of phosphorene nanoribbon as shown in Fig. 7(a). The HOMO and LUMO orbitals and differences between their energies (E_g) and the values of Fermi energies (E_f) of UPNT and CPNT conFigurations are computed and summarized in Table 2. The computed parameters and their comparison show that the CPNT and UPNT conFigurations show a significant difference in their electronic properties. In this work we assume that each unit of the UPNT and CPNT structures are constructed of 24 atoms of carbon across the

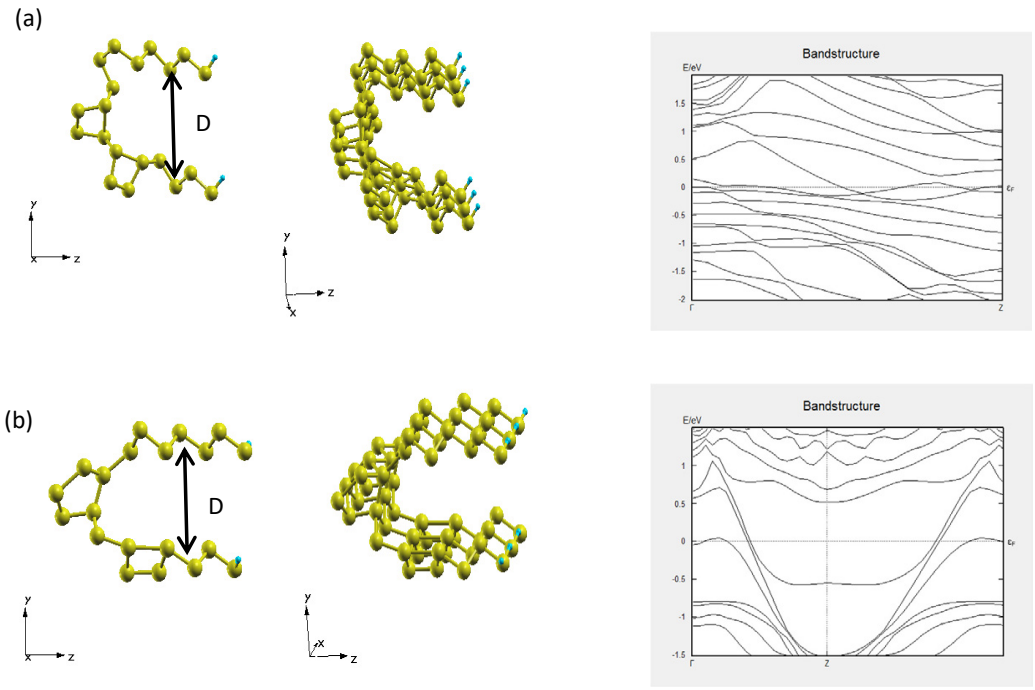

Fig. 6. Phosphorene nanoribbon atomic structure and energy band structure diagram of different arm distances: a) D= 8.44 Aº, E_f = -3.87 eV , E_g =0 eV b) D=5.83 Aº, E_f = = -4.26 eV , E_g =0 eV.

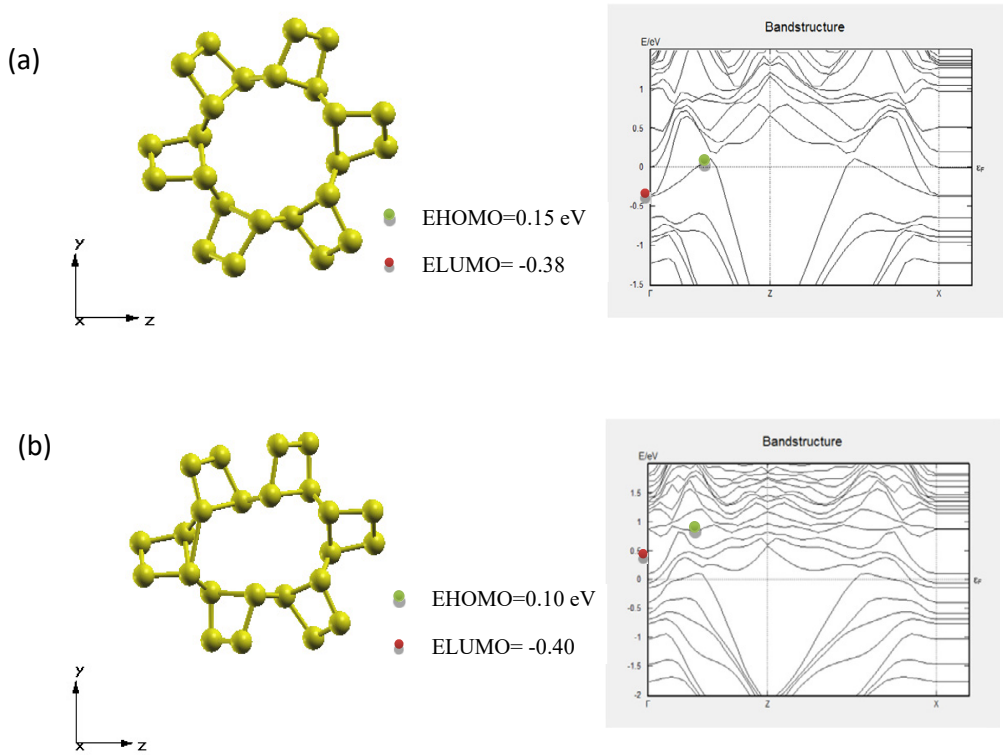

Fig. 7. a) CPNT with its energy diagram and b) UPNT with its energy diagram.

Table2. Comparison of energy parameters of CPNT and UPNT.

	Ef (eV)	Eg (eV)	Ehomo (eV)	Elumo (eV)
CPNT	-2.86	0	-2.20	-2.85
UPNT	-2.89	0	-2.41	-2.78

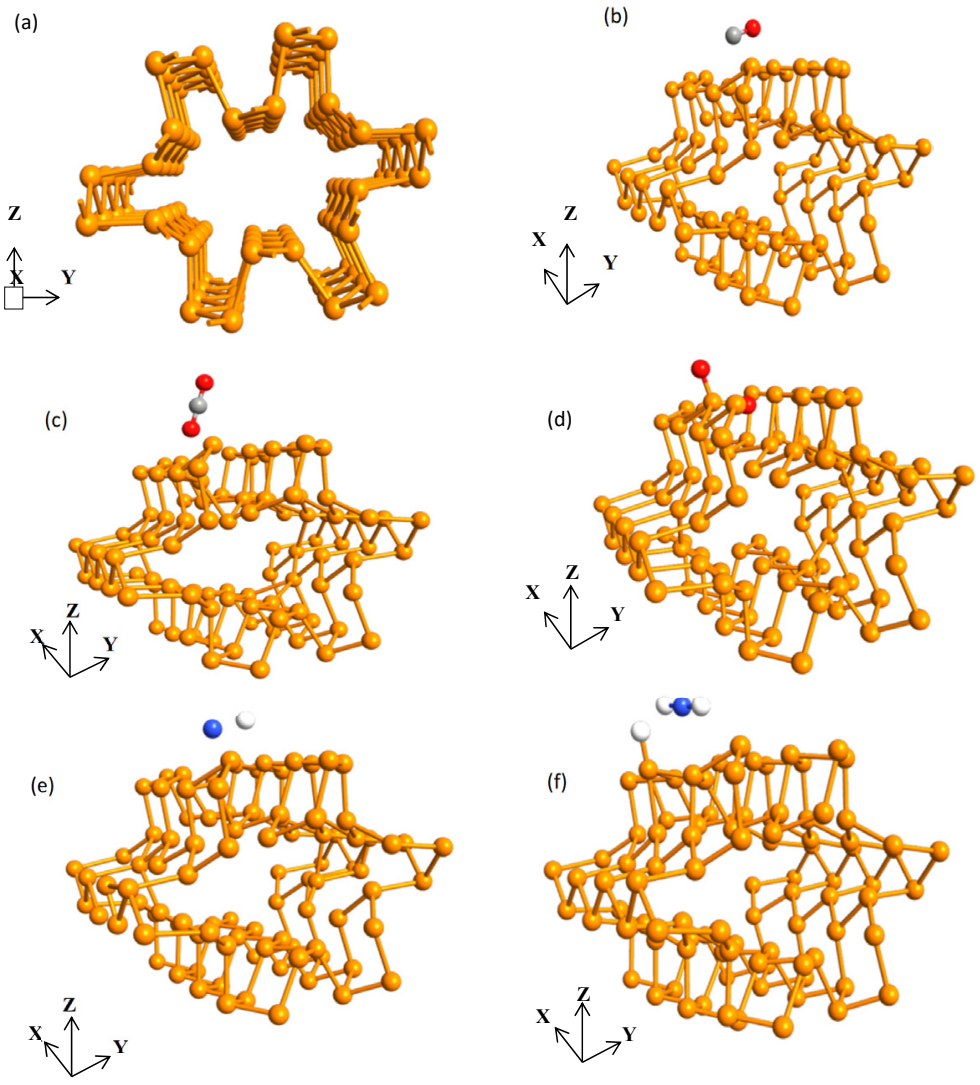

Fig. 8. Atomic structure of UPNTs: a) without gas adsorption, b) with CO gas molecule, c) with CO_2 gas molecule, d) with O_2 gas molecule, e) with NH gas molecule, f) with NH_3 gas molecule, (the gray, white, red and blue circles correspond to Carbon, Hydrogen, Oxygen and Nitrogen atoms, respectively).

width of the nanoribbon. Comparison of energy properties of CPNT and UPNT are shown in Table 2.

PNT Gas sensor

At this stage, we examine the effect of adsorption of different gases onto the UPNT and the CPNT. We also investigate the structural deformation due to the presence of gases. Therefore, UPNT and CPNT structures respectively used to explore their behavior due to adsorption of O_2, CO, CO_2, NH_3, and NH gases. Supposing to

achieve the most stable atomic conFiguration, first, the gases molecules of O_2, CO, CO_2, NH_3 and NH with different initial orientations are turned around alternatively and connected at different locations on the PNT surface. Then, the structures are also relaxed in the same way using Quantum Espresso 5.3.0 through the initial relaxed structures; we should notice that the structure with the least total energy is the most stable one.

The compound structures including the consolidation of UPNT with gas molecules and the CPNT also with gas molecules are introduced in the following subsections. Additionally, the electronic characteristics and sensing characteristics of gas sensors are inspected in subsection 3.4. We present all the relaxed UPNT and CPNT atomic structures in the existence of different gases molecules in Fig. 8 and Fig. 9. More over the

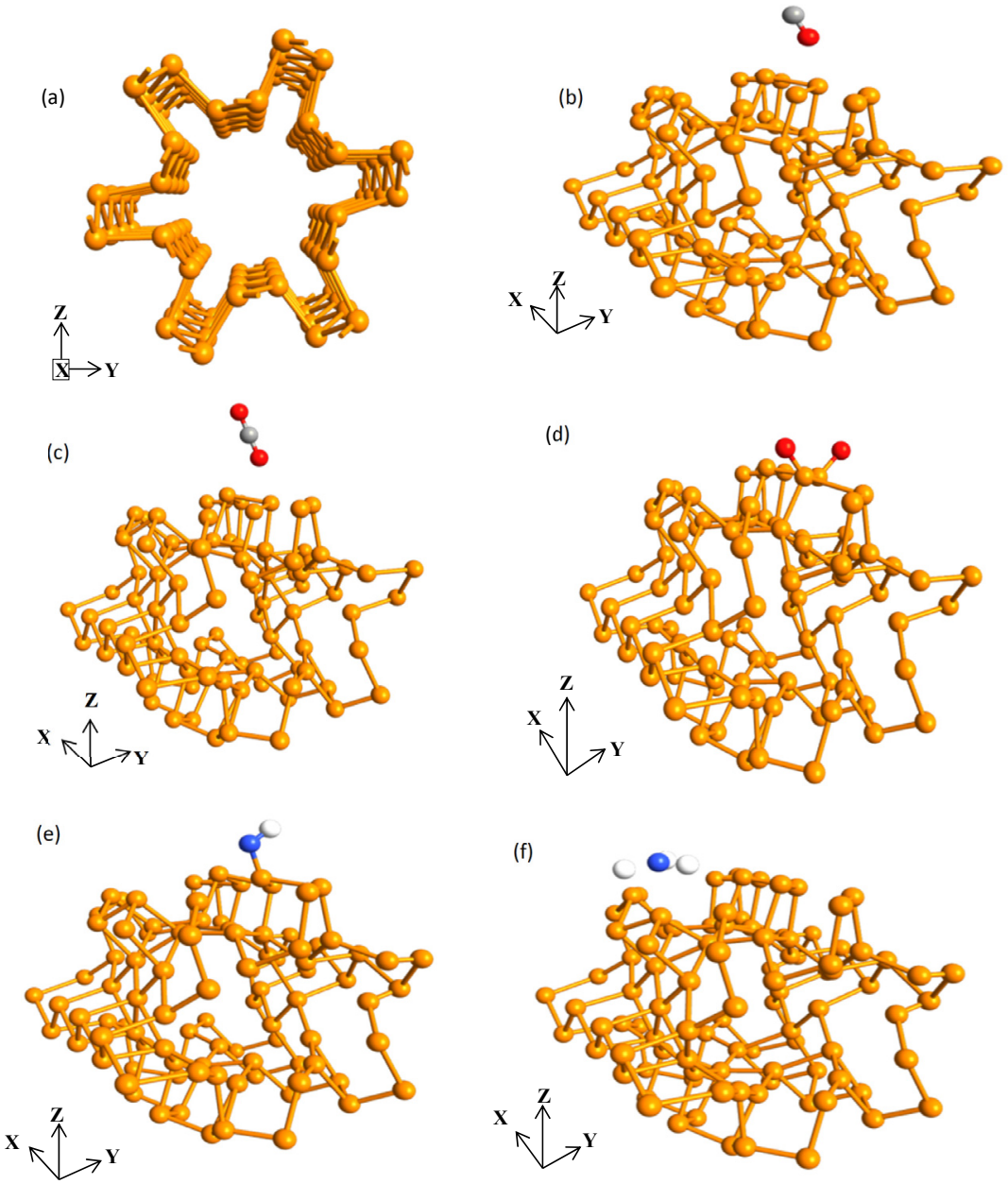

Fig. 9. Atomic structure of CPNTs: a) without gas adsorption, b) with CO gas molecule, c) with CO_2 gas molecule, d) with O_2 gas molecule, e) with NH gas molecule, f) with NH_3 gas molecule after relaxation, (the gray, white, red and blue circles correspond to Carbon, Hydrogen, Oxygen and Nitrogen atoms, respectively).

Table3. The position of the atoms relative to each other in different configurations.

Configuration	P-P distance (Aº)	Interaction distance (Aº)	Angle(degree)
CPNT	2.24	-	-
CPNT-CO	2.21	2.61	79.20
CPNT- CO_2	2.20	2.52	72.34
CPNT- O_2	2.19	1.51	Link has been established
CPNT-NH	2.22	1.59	47.11
CPNT- NH_3	2.16	2.29	Link has been established
UPNT	2.26	-	-
UPNT - CO	2.24	2.27	25.26
UPNT- CO_2	2.20	2.90	46.21
UPNT- O_2	2.25	1.49	Link has been established
UPNT-NH	2.24	2.27	24.22
UPNT NH_3	2.17	1.50	Link has been established

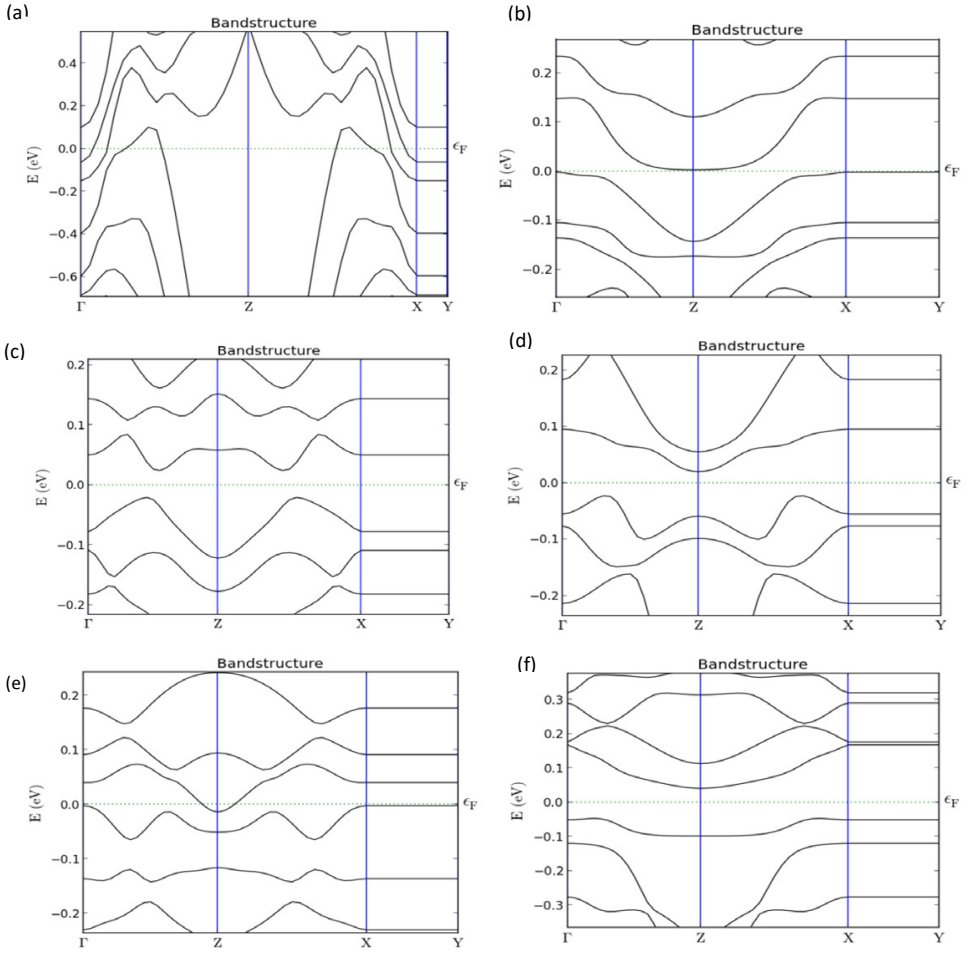

Fig. 10. Band diagrams of the UPNT: a) without gas adsorption, b) with CO gas molecule, c) with CO_2 gas molecule, d) with O_2 gas molecule, e) with NH gas molecule and f) with NH_3 gas molecule after relaxation.

calculated bonding length and angles between P-P atoms and P-gases atoms before and after gas absorption are listed in Table 3, where all the structures have been fully relaxed. Fig. 8(a) shows the atomic structure of UPNT without gas adsorption. For the CO and CO_2 adsorption onto UPNT and CPNT, the carbon atom relaxes at the center of the puckered honeycomb as shown in Figs. 8(b, c) and Figs. 9(b, c). In contrast, in the case of NH molecule, it moves to the top position of a P atom while interaction of the N and H atoms is changed and separated as shown in Fig. 8(e) and Fig. 9(e). However, in the case of O_2 molecule, both oxygen atoms bond with the P atoms because of

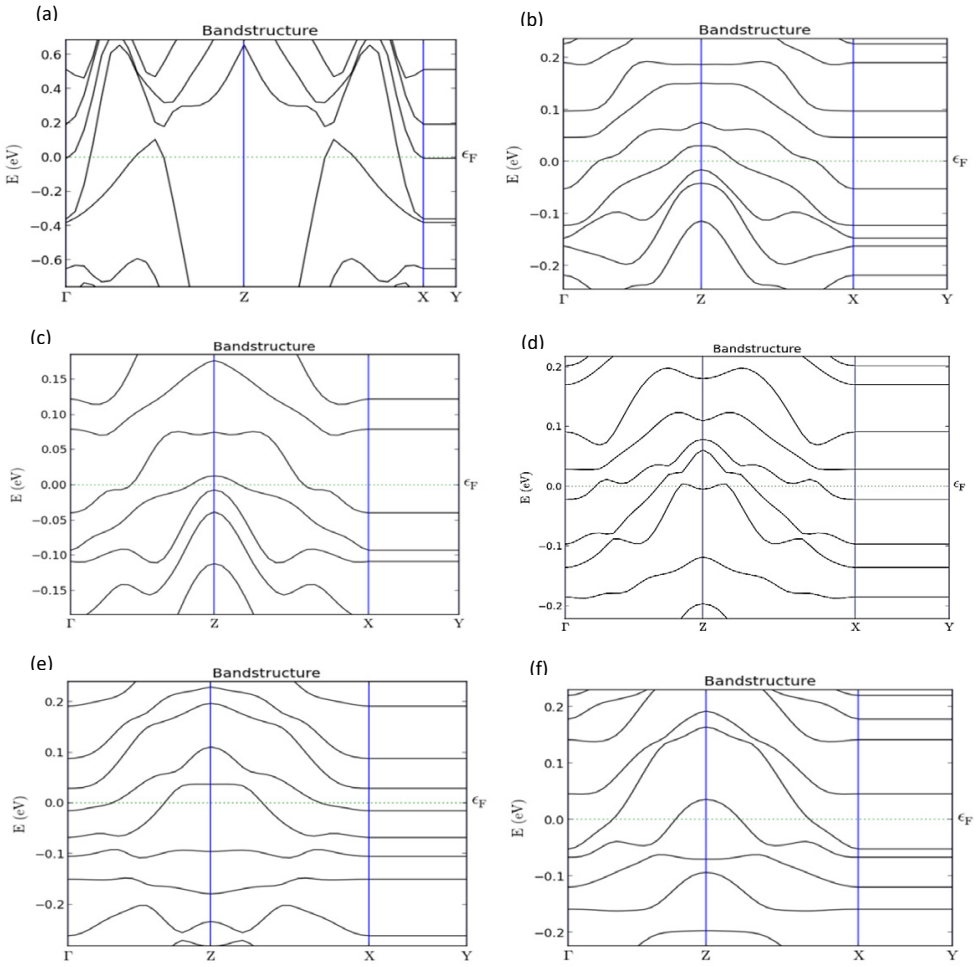

Fig. 11. Band diagrams of the CPNT: a) without gas adsorption, b) with CO gas molecule, c) with CO_2 gas molecule, d) with O_2 gas molecule, e) with NH gas molecule and f) with NH_3 gas molecule after relaxation

the lack of dangling bonds and they rest above the PNT structure as shown in Fig. 8(d) and Fig. 9(d). Similarly, NH_3 molecule relaxes above the PNT structure with an adsorption distance of 2.16Å and 2.17Å for the CPNT and UPNT, respectively. In this case, as shown in Fig. 8(f), the N atom is placed at the center of the puckered honeycomb. Of course, for adsorption of NH_3 molecule onto the CPNT, one of the H atoms is separated from the NH_3 molecule and placed at the closest distance to the phosphorus atom as shown in Fig. 9(f). To visualize the angle, the shape must be rotated in a way that the phosphorus atom to be placed in line with one of the gas atoms. Therefore, in CPNT- O_2, CPNT- NH_3, UPNT- O_2 and UPNT- NH_3 conFigurations, the link between phosphorous atom and oxygen or hydrogen atom is established, where the calculated angle is zero degree. For CPNT-CO, CPNT- CO_2, CPNT-NH, UPNT–CO, UPNT-CO_2, UPNT-NH conFigurations, the bonding angles are, 79.20, 72.34, 47.11, 25.26, 46.21, 24.22 degrees respectively that are shown in Table 3.

Analysis of band structures

Now, it is useful to study the impacts of gas absorption on the electronic properties of the UPNT and CPNT. Figs. 10(a-f) and Figs. 11(a-f) shows the band diagrams and energy states of the UPNT and CPNT respectively with and without the adsorption of CO, CO_2, O_2, NH_3 and NH gases molecules. The gas adsorption onto the UPNT and CPNT structures affect the devices properties, which are listed in Table 4.

The charge transfer between the UPNT and CPNT and gases given in Table 4 are computed utilizing charge density analysis. As shown in

Table 4, some of the calculated numbers of transfer charges are negative. The negative sign of transferred charge is because of the direction of charge transfer that is from the phosphorene structure to the gas molecule.

Density of states (DOS)

Now, it is interested to investigate the influence of gas adsorption on the electronic properties of UPNT and CPNT. We depicted in Figs. 12(a-f) and Figs. 13(a-f) the total density of states (DOS) of the

Table 4. Bandgap energies, Transferred charge, HOMO, LUMO and Fermi level of gas adsorption onto UPNT and CPNT.

Configuration	E_g (eV)	Q(e)	E_{HOMO} (eV)	E_{LUMO} (eV)	E_f (eV)
UPNT with CO	0.01	0.003	-3.28	-3.27	-3.28
UPNT with CO_2	0.04	-0.11	-3.24	-3.19	-3.22
UPNT with NH	0	0.23	-3.64	-3.65	-3.64
UPNT with NH_3	0.09	0.16	-3.34	-3.25	-3.30
UPNT with O_2	0.04	0.25	-3.31	-3.27	-3.29
CPNT with CO	0	-0.06	-3.27	-3.30	-3.35
CPNT with CO_2	0	-0.10	-3.29	-3.29	-3.36
CPNT with NH	0	0.05	-3.30	-3.38	-3.41
CPNT with NH_3	0	0.03	-3.22	-3.33	-3.38
CPNT with O_2	0	0.22	-3.25	-3.30	-3.33

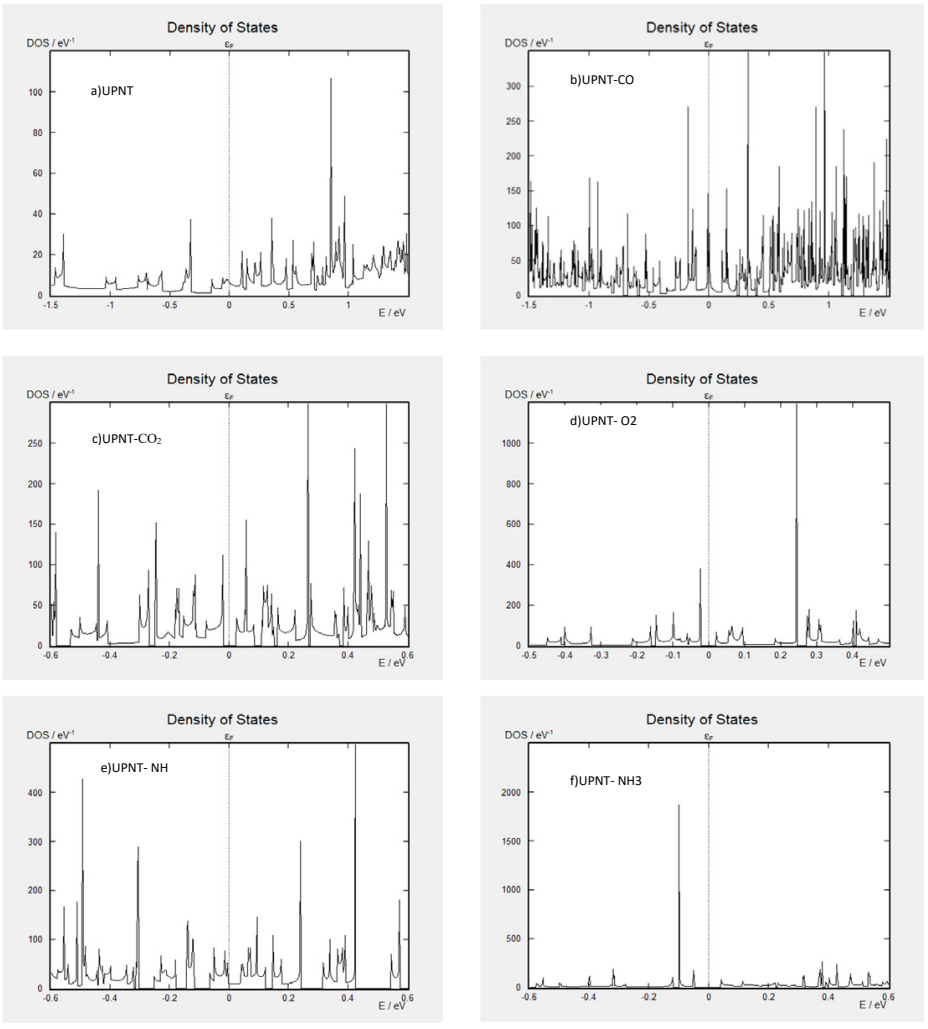

Fig. 12. Densities of states of the UPNT: a) without gas adsorption, b) with CO gas molecule, c) with CO_2 gas molecule, d) with O_2 gas molecule, e) with NH gas molecule and f) with NH_3 gas molecule after relaxation.

UPNT and CPNT, respectively, before and after a set of gases such as CO, CO_2, NH, NH_3 and O_2 gases molecules adsorption.

As illustrated in Fig. 12(b), the presence of CO gas molecule causes the UPNT to the accumulated some significant states around the Fermi level which increases the conductivity, consequently. In Figs. 12(c, d, e), DOS near the Fermi level of the UPNT in presence of CO_2, O_2 and NH gas molecules surge slightly. This means that the conductivity of the UPNT can be increased slightly because of CO_2, O_2 and NH gas molecules adsorption. Similarly, Fig. 12(f) demonstrates DOS due to absorption of NH_3 molecules onto the UPNT, where a sharp increase of DOS around the Fermi level makes the UPNT more metallic. In fact, accumulation of remarkable states of electrons around the Fermi level in the presence of NH_3 gas molecule can lead to a considerable alteration in its conductivity.

As depicted in Figs. 13(b, c), presence of CO, CO_2

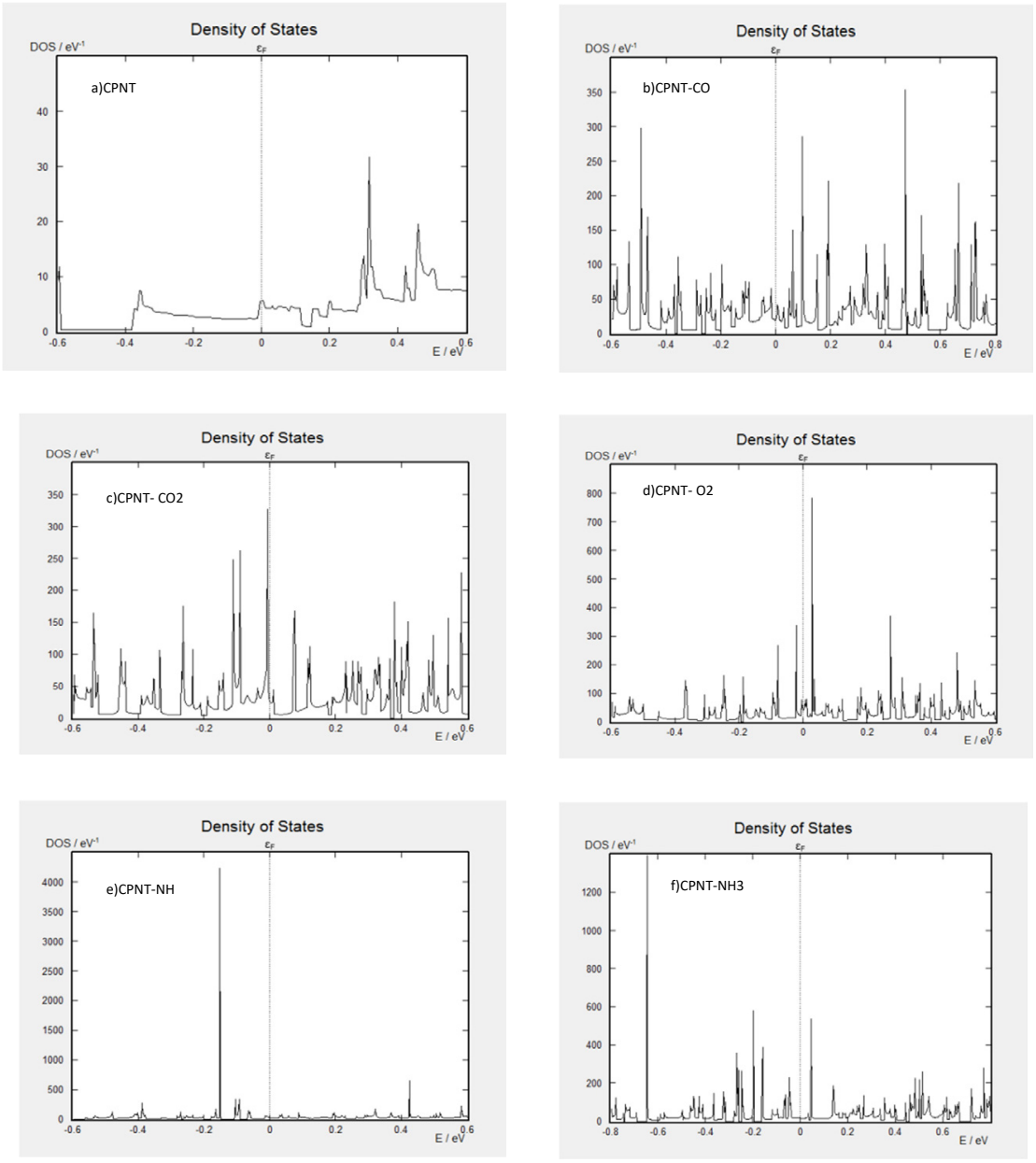

Fig. 13. Densities of states of the CPNT: a) without gas adsorption, b) with CO gas molecule, c) with CO_2 gas molecule, d) with O_2 gas molecule, e) with NH gas molecule and f) with NH_3 gas molecule after relaxation.

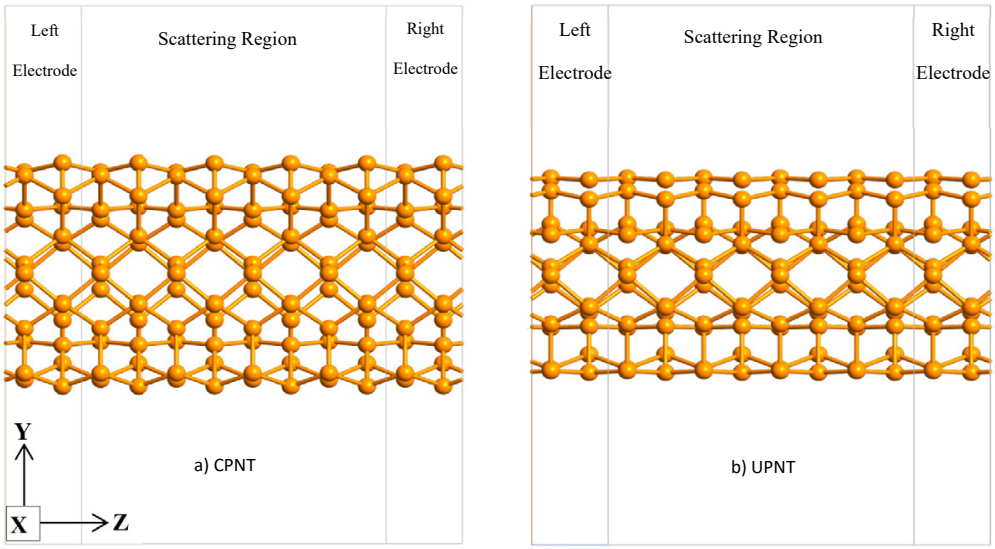

Fig. 14. The phosphorene-based resistance sensor is constructed of two semi-infinite PNT that act as electrodes and a finite PNT for gas adsorption which acts as a channel, a) the CPNT based sensor and b) the UPNT based sensor with contacts.

gases molecules doesn't change the states near the Fermi level of the CPNT and its conductivity, consequently. On the other hand, the DOS of CPNT in presence of O_2, NH and NH_3 gases molecules that shown in Figs. 13(d, e, f) illustrate a huge peak appearing around the Fermi level. Therefore, the DOS of the above cases pointed out that specially the CPNT-NH emerges highly metallic and can lead to a notable raise in conductivity of the system. In addition, the NH_3 adsorption onto UPNT illustrates that its conductivity can increase. Hence, it can be concluded that CPNT is sensitive to the existence of NH gas molecule and UPNT is sensitive to the existence of NH_3 gas molecule.

The Current-Voltage characteristic and sensitivity

The adsorption of gases onto PNTs persuade charge transfer and definitely influence the resistivity of the system, thus this property acts as a marker for gas sensors. To evaluate the capabilities of UPNT and CPNTs as a gas sensor, we used the NEGF technique to compute the charge transfer and the corresponding current-voltage (I-V) relation after and before each gas adsorption and allowing monitoring of the resistivity alteration.

As shown in Figs. 14(a, b), 1*1*4 supercell is applied for both of the left and right electrodes in CPNT and UPNT based sensors respectively, while the center part consists of 1*1*4 surpercell and scattering is considered there. This supercell atomic conFiguration is exactly same as that acquired from the relaxed structure processes. The relaxed structures are used in the electronic calculations at different bias voltages from 0V to 0.8V by 0.1V intervals. In Figs. 15(a, b) we have presented the I-V curves of UPNT and CPNT with and without gases adsorption respectively. When a positive bias voltage is applied to the right electrode, the Fermi level of the right electrode shifts downward with respect to that of the left electrode and electrons flow to the right. The I-V characteristics of UPNT and CPNT in Figs. 15(a, b) illustrate that the threshold voltage of UPNT (V_{th}=0.1V) is less than that of the CPNT (V_{th}=0.6V) without applying gas molecules, which means that the CPNT behaves more semiconducting than the UPNT. Also, the I-V characteristics plotted in Fig. 15(a) show that, after adsorption of NH and NH_3 the currents of UPNT contain greater changes comparing to that of the pristine UPNT. Meanwhile, these changes were predictable by considering the corresponding DOS curves.

Resistive gas sensor is based on I-V curve of an atomic structure in both conditions, before and after gas adsorption. In this kind of sensor the sensitivity to the existence of a gas is evaluated by computing change in the current, ΔI, utilizing the following formula: $\Delta I = I_{PNT + gas} - I_{PNT}$. Accordingly, the total sensitivity of PNTs atomic structures is gained from their current alterations based on

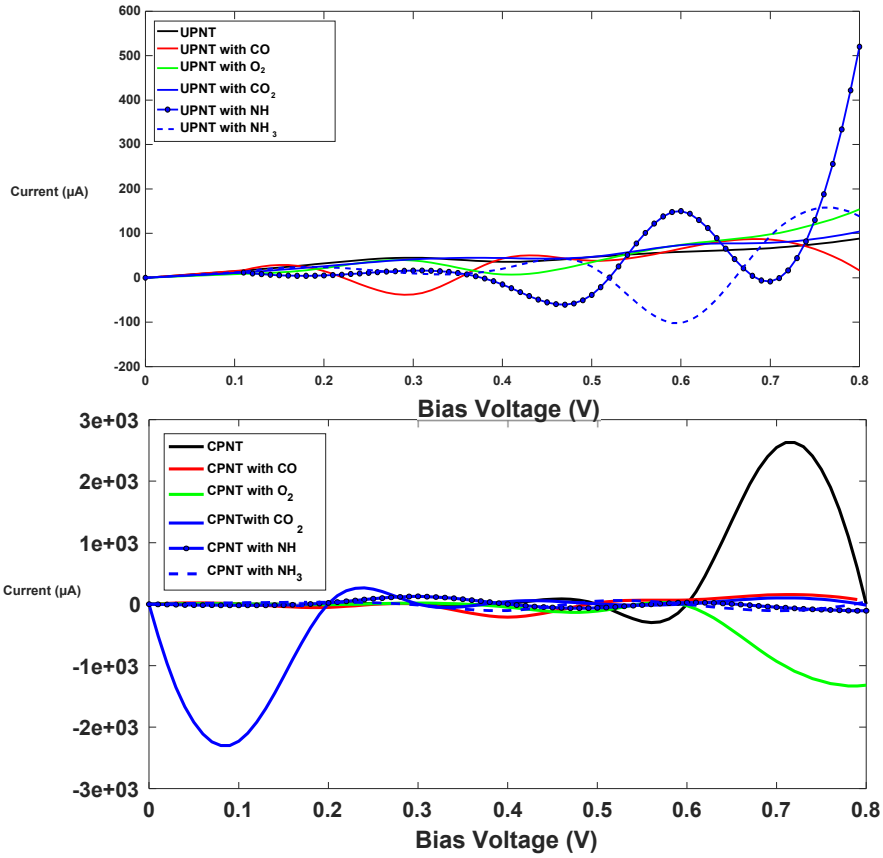

Fig. 15. I-V characteristics of: a) UPNT and b) CPNT in presence of CO, O_2, CO_2, NH and NH_3 gases.

absorption of CO, CO_2, O_2, NH and NH_3 gases atoms at variant bias voltages. All current changes and sensitivities due to gas adsorption are illustrated and compared in Fig. 16. At this stage, we should pay attention to the selectivity of sensor in addition to its sensitivity. In fact, in many cases selectivity can be more helpful than sensitivity. In other word, an ideal gas sensor should be sensitive to the existence of a specific gas, while it should not be sensitive to other ambient gases at the same time. As Fig. 16 (a) depicted, at bias voltage of 0.7V notable variations occurred in the current of CPNT in the existence of CO, CO_2 , O_2, NH and NH_3 gases molecules, but the amounts of changes are almost in the same value and orders. However, at bias voltage of 0.1V the CPNT is less sensitive to the existence of the gases CO, O_2, NH and NH_3 while it is more sensitive to the existence of gas CO_2, which means it is selective only for CO_2. Moreover, Fig. 16(b) illustrates that the UPNT is much more sensitive to NH and NH_3 gases in comparison to the CO, CO_2 and O_2 gases. As shown in Fig. 16(b), the sensitivity of UPNT to NH molecules increases when the bias voltage goes up and it turns into a considerable value at bias voltage of 0.8v. Also we can deduce that UPNT is relatively selective for NH gas at bias voltage of 0.6V and for CO gas at bias voltage of 0.3V. It is noticeable that applying of an electric field (bias voltage) along an atomic structure changes its energy band dramatically [28]. This consequently alters the current-voltage characteristics of the nano sensors as clarified in this work. Nevertheless, it is important to know that changes in the I-V characteristics of presented device don't follow the classical behaviors, which is due to its quantum-mechanical properties. Also as Fig. 16(b) shows, the UPNT structure is more sensitive to NH adsorption at 0.8V bias voltage. Eventually, it is also shown that the UPNT structure as a NH gas sensor has an impressive benefit because of its sensitivity and selectivity properties. This happens due to its very small amount of current in lack of gas molecules and a notable current in the existence of NH molecules at

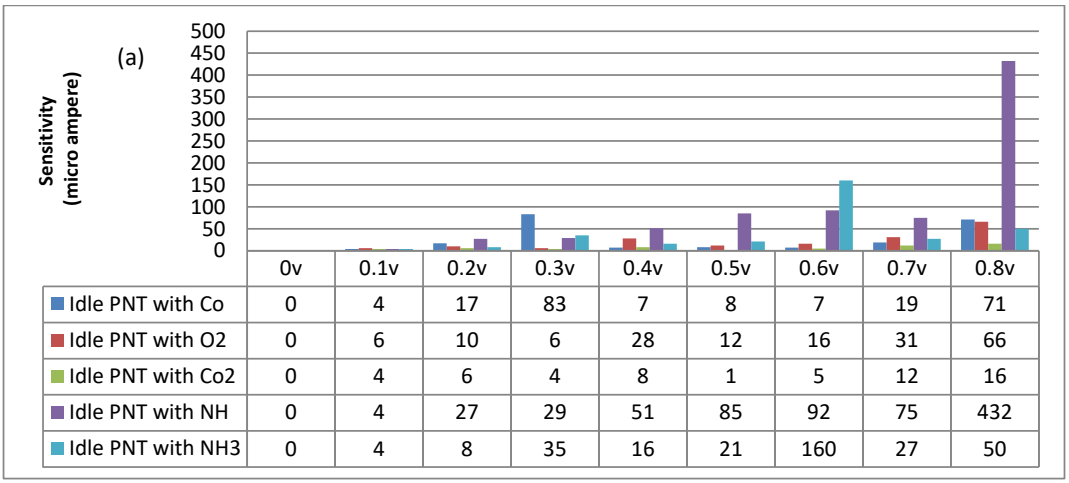

	0v	0.1v	0.2v	0.3v	0.4v	0.5v	0.6v	0.7v	0.8v
Idle PNT with Co	0	4	17	83	7	8	7	19	71
Idle PNT with O2	0	6	10	6	28	12	16	31	66
Idle PNT with Co2	0	4	6	4	8	1	5	12	16
Idle PNT with NH	0	4	27	29	51	85	92	75	432
Idle PNT with NH3	0	4	8	35	16	21	160	27	50

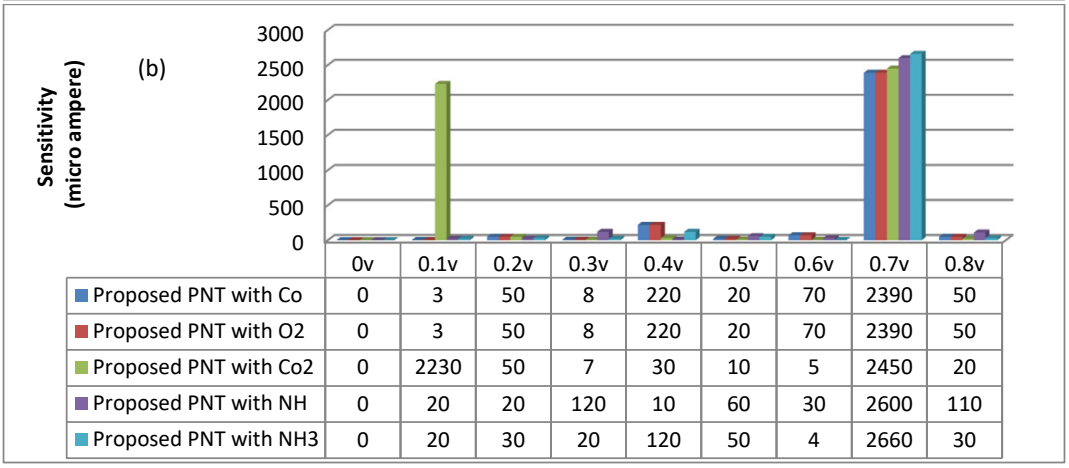

	0v	0.1v	0.2v	0.3v	0.4v	0.5v	0.6v	0.7v	0.8v
Proposed PNT with Co	0	3	50	8	220	20	70	2390	50
Proposed PNT with O2	0	3	50	8	220	20	70	2390	50
Proposed PNT with Co2	0	2230	50	7	30	10	5	2450	20
Proposed PNT with NH	0	20	20	120	10	60	30	2600	110
Proposed PNT with NH3	0	20	30	20	120	50	4	2660	30

Fig. 16. The sensitivity of: a) CPNT structure and b) UPNT structure in presence of CO, O_2, CO_2, NH and NH_3 gas molecules.

bias of 0.8V. In addition, UPNT shows that besides good selectivity and high sensitivity, it consumes low power in normal circumstances.

CONCLUSION

In this paper, the electrical properties and current characteristics of zigzag phosphorene nanoribbon (ZPNR) structures with different number of atoms in width were investigated. Then, by folding the ZPNR structure, the effect of changes in the arms and the longitudinal distance of the folded arms on band structures were investigated. According to the results we obtained two different structures of phosphorene nanotube (PNT), one obtained by connecting two folded structures and the other by rolling a PNR with a specified number of atoms in the width. The first one is named unconventional phosphorene nanotube (UPNT) and the second one named conventional phosphorene nanotube (CPNT). We eventually exposed these two structures to different gases molecules. The influence of CO, CO_2, O_2, NH and NH_3 gases adsorptions on the electronic properties of UPNT and CPNT have been studied based on the DFT in combination with the NEGF method. Moreover, I-V characteristics indicated the change in the current across the two probe phosphorene molecular device upon the adsorption of CO, CO_2, O_2, NH and NH_3 molecules. The selectivity issues of the CO, CO_2, O_2, NH and NH_3 gases in environmental condition are also studied. These results confirm the I-V characteristics of the structures, where the changes in DOS change the current consequently. It is also concluded that the UPNT device can be used to detect the gas presented in the atmosphere. The results show high sensitivity to adsorption; moreover it remarkably demonstrates excessive selectivity in presence of gas molecules

which cause variations in the transport behavior, especially for NH adsorption on UPNT.

CONFLICT OF INTEREST

Authors have no conflict of interest.

REFERENCES

[1] Coleman J. N., Lotya M., O'Neill A., Bergin Sh. D., King P. J., Khan U., Young K., Gaucher A., De S., Smith R. J., Shvets I. V., Arora S. K., Stanton G., Kim H-Y., Lee K., Tae Kim G., Hallam T., Boland J. J., Wang J. J., Donegan J. F., Grunlan J. C., Moriarty G., Shmeliov A., Nicholls R. J., Perkins J. M., Grieveson E. M., Theuwissen K., McComb D. W., Nellist P. D., Nicolosi V., (2011), Two-dimensional nanosheets produced by liquid exfoliation of layered materials. *Science.* 331: 568–571.

[2] Geim A. K., (2009), Graphene: Status and prospects. *Science*. 324: 1530–1534.

[3] Stankovich S., Dikin D. A., Dommett G. H. B., Kohlhaas K. M., Zimney E. J., Stach E. A., Piner R. D., Nguyen S. B. T., Ruoff R. S., (2006), Graphene-based composite materials. *Nature*. 442: 282–286.

[4] Yin X., Ye Z., Chenet D. A., Ye Y., O,Brien K., Hone J. C., Zhang X., (2014), Edge nonlinear optics on a MoS_2 atomic monolayer. *Science.* 344: 488–490.

[5] Radisavljevic B., Radenovic A., Brivio J., Giacometti V., Kis A., (2011), Single-Layer MoS_2 Transistors. *Nat. Nanotechnol.* 6: 147−150.

[6] Butler S. Z., Hollen S. M., Cao L., Cui Y., Gupta G. A., Gutierrez H. R., Heinz T. F., Hong S. S., Houang J., (2013), Progress, challenges, and opportunities in two-dimensional materials beyond graphene. *ACS Nano.* 7: 2898-2926.

[7] Neto A. H., Guinea F., Peres N. M. R., Novoselov K. S., Geim A. K., (2009), The electronic properties of graphene. *Rev. Mod. Phys.* 81: 109-162.

[8] Wang Q. H., Kalantar-Zadeh K., Kis A., Coleman J. N., Strano M. S., (2012), Electronics and optoelectronics of two-dimensional transition metal dichalcogenides. *Nat. Nanotechnol.* 7: 699-712.

[9] Sruthy P. C., Nagarajan V., Chandiramouli R., (2020), Interaction studies of kidney biomarker volatiles on black phosphorene nanoring: A first-principles investigation. *J. Molec. Graph. Model.* 97: 107-115.

[10] Liu H., Neal A. T, Zhu Z., Tománek D., Ye P. D., (2014), Phosphorene: An unexpected 2D semiconductor with a high hole mobility. *ACS Nano*. 8: 4033-4041.

[11] Reich E. S., (2014), Phosphorene excites materials scientists. *Nature*. 19: 506-517.

[12] Takao Y., Asahina H., Morita A., (1981), Electronic sructure of black phosphorus in tight binding approach. *J. Phys. Soc. Jpn.* 50: 3362-3369.

[13] Appalakondaiah S., Vaitheeswaran G., Lebègue S., Christensen N. E., Svane A., (2012), Effect of van der waals interactions on the structural and elastic properties of black phosphorus. *Phys. Rev. B*. 86: 035105-035108.

[14] Lama K., Liangb G., (2008), An ab initio study on energy gap of bilayer graphene nanoribbons with armchair edges. *Appl. Phys. Lett.* 92: 223106-223110.

[15] Dai J., Zeng X. C., (2014), Bilayer phosphorene: Effect of stacking order on bandgap and Its potential applications in thin-film solar cells. *J. Phys. Chem. Lett.* 5: 1289-1293.

[16] Kou L., Frauenheim T., Chen C., (2014), Phosphorene as a superior gas sensor: Selective adsorption and distinct I–V response. *J. Phys. Chem. Lett.* 5: 2675–2681.

[17] Giannozzi P., Baroni S., Bonini N., Calandra M., Car R., Cavazzoni C., Ceresoli D., Chiarotti G. L., Cococcioni M., Dabo I., (2009), QUANTUM ESPRESSO: A modular and open-source software project for quantum simulations of materials. *J. Phys. Condens. Matter*. 21: 395502-395508.

[18] Vanderbilt D., (1990), Soft self-consistent pseudopotentials in a generalized eigenvalue formalism. *Phys. Rev. B*. 41: 7892-7896.

[19] Perdrew J. P., Chevary J. A., Vosko S. H., Jacson K. A., Pederson M. R., Singh D. J., Fiolais C., (1992), Atoms, molecules, solids, and surfaces: Applications of the generalized gradient approximation for exchange and correlation. *Phys. Rev. B*. 46: 66-71.

[20] Ramasubramaniam A., (2010), Electronic structure of oxygen-terminated zigzag grapheme nanoribbos: A hybrid density functional theory study. *Phys. Rev. B.* 81: 25413-25416.

[21] Omidvar A., Mohajeri A., (2014), Edge functionalized graphene nanoflakes as selective gas sensor sensors and actuators. *B: Chemical.* 202: 622-630.

[22] Wang H., Li X., Li P., Yang J., (2017), Phosphorene: A two dimensional material with a highly negative Poisson's ratio. *Nanoscale.* 9: 850-855.

[23] Zhang Z., Cheng M-Qi ., Chen Q., Wu H-Yu., Hu W., Peng P., Huang G.F., Huang W.Q., (2019), Monolayer phosphorene–carbon nanotube heterostructures for photocatalysis: Analysis by density functional theory. *Nanosc. Res. Lett.* 14: Article number: 233 .

[24] Huang G., Xing Z. W., Xing D. Y., (2015), Prediction of superconductivity in Li-intercalated bilayer phosphorene. *Appl. Phys. Lett.* 106: 107-113.

[25] Han C. Q., Yao M. Y., Bai X. X., Miao L., Zhu F., Guan D. D., Wang Sh., Gao C. L., Liu C., Qian D., Liu Y., Jia J-F., (2014), Electronic structure of black phosphorus studied by angle-resolved photoemission spectroscopy. *Phys. Rev. B*. 90: 085101-085106.

[26] Monkhorst H. J., Pack J. D., (1976), Special points for brillouin-zone integrations. *Phys. Rev. B.* 13: 5188-5193.

[27] Gajdos M., Hummer K., Kresse G., Furthmuller J., Bechstedt F., (2006), Linear optical properties in the projector-augmented wave methodology. *Phys. Rev. B.* 73: 045112-045118.

[28] Paier J., Marsman M., Kresse G., (2008), Dielectric properties and excitons for extended systems from hybrid functional. *Phys. Rev. B.* 78: 121-201.

[29] Brandbyge M., Mozos J. L., Ordejon P., Taylorand J., Stokbro K., (2002), Density-functional method for nonequilibrium electron transport. *Phys. Rev. B.* 65: 165401-165406.

[30] Aghdasi P., Ansari R., Rouhi S., Yousefi Sh., Goli M., Soleimani H. R., (2021), Investigating elastic and plastic characteristics of monolayer phosphorene under atomic adsorption by the density functional theory. *Phys. B: Cond. Matt.* 600: 412603-412606.

[31] Topsakal M., Bagci V. M., Ciraci S., (2010), Current-voltage (I-V) characteristics of armchair graphene nanoribbons under uniaxial strain. *Phys. Rev. B.* 81: 205437-205442.